Int. J. Heat Mass Transfer. Vol. 36, No. 3, pp. 553–563, 1993
Printed in Great Britain

0017–9310/93 $6.00+0.00
Pergamon Press Ltd

The influence of tube layout on flow and mass transfer characteristics in tube banks in the transitional flow regime

TATSUO NISHIMURA
Department of Mechanical Engineering, Yamaguchi University, Ube 755, Japan

and

HISAYOSHI ITOH and HISASHI MIYASHITA
Department of Materials Science and Engineering, Toyama University, Toyama 930, Japan

(*Received* 18 *September* 1991 *and in final form* 12 *May* 1992)

Abstract—Flow and mass transfer characteristics in tube banks are investigated in the transitional flow regime at intermediate Reynolds numbers. The tube arrays considered are a staggered tube array and an in-line tube array with longitudinal and transverse pitch-to-diameter ratios of two. The flow is steady at the entrance of the tube banks, but becomes oscillatory downstream of an onset location of vortex shedding. This location moves upstream with increasing Reynolds number, and the upstream development of flow transition is much faster for the staggered array than the in-line array. Therefore, the row-by-row variation of the mass transfer rate is small for the staggered array but considerable for the in-line array. The mass transfer for the staggered array is sensitive to the unsteady wakes of the preceding row tubes, while the surface shear stress is insensitive to such wakes. However, for the in-line array the mass transfer and shear stress are both sensitive to the unsteady wakes.

1. INTRODUCTION

MANY DESIGNS exist for heat exchangers involving a bank of tubes in a fluid crossflow. Depending on applications and design criteria, there are many possibilities for the layout of tubes in an array. A heat exchanger designer, therefore, needs access to the largest possible database in order to choose the optimal design option. Recently, due to the rapid development of computers, numerical analysis has come to be used for design of engineering devices as well as experiments.

Several reviews of the literature on fluid flow and heat transfer in tube banks have been published [1–3]. Most of the numerical studies were limited to steady laminar flow conditions [4, 5]. It is commonly observed in heat exchanger cores that even in the laminar flow regime the flow may be unsteady because of vortex shedding. At high Reynolds numbers, the downstream region in the core is characterized by turbulent flow [6–9]. Although numerical analysis by computer has a bright future in the design of engineering devices, except for certain turbulence models [10, 11], it is not yet well established due to unusual complexity of flow phenomena. Therefore, a detailed set of experimental data is needed for testing and refining the numerical analysis.

In this study, we investigate experimentally fluid flow and mass transfer in tube banks for a staggered array and an in-line array at the transition from steady to unsteady flow. Such transitional flow appears to involve a remarkable change in heat and mass transfer rates, as suggested by Zukauskas and Ulinskas [12]. On the basis of many experiments, they reported that, for laminar flow, a staggered array has a higher heat transfer coefficient in the fully developed flow region of tube banks than an in-line array with the same pitch-to-diameter ratio, while for turbulent flow, the effect of tube layout is minimal.

Previous studies on the transitional flow regime including laminar flow provide only fragmentary information. Nieva and Böhm [13, 14] presented local mass transfer coefficients around a tube placed in a tube bank for four different pitches at intermediate Reynolds numbers. However, the effect of flow transition on local mass transfer rates was not made clear, because the variation of flow patterns with Reynolds number was not considered. Weaver and Abd-Rabbo [15] observed flow patterns for an in-line array of four tube rows over a wide range of Reynolds number, and flow visualizations showed that flow development is a function of not only Reynolds number but also the row number of tubes. Recently, Nishimura *et al.* [16] studied numerically and experimentally the effect of tube layout on the surface shear stress distribution for steady laminar flow. They found a large difference in the shear stress between the staggered and in-line arrays at the front of the tube but almost no difference at the rear.

Although not directly related to the present work,

NOMENCLATURE

A	area of mass transfer surface
B	surface velocity gradient
C_b	concentration of ferricyanide ion
D	diameter of tube
d	diameter of electrode
F	Faraday's constant
f	frequency of vortex shedding
i_d	diffusional current
k	mass transfer coefficient
N	row number in the streamwise direction
Nu	Nusselt number
P	pitch of tubes
Pr	Prandtl number
Re	Reynolds number, $U_i D/\nu$
Re_c	Reynolds number at the transition from steady to unsteady flow
Re_{max}	Reynolds number, $U_{max} D/\nu$
Sc	Schmidt number, ν/φ
Sh	Sherwood number, kD/φ
St	Strouhal number, fD/U_i
T	period of vortex shedding, $1/f$
U_i	upstream velocity of tube banks
U_{max}	velocity at the minimum flow area between tubes.

Greek symbols

ζ_s	dimensionless surface vorticity, $BD/(2U_i)$
θ	angle of circumference measured from stagnation point
μ	viscosity
ν	kinematic viscosity
τ_s	surface shear stress, μB
φ	molecular diffusivity of ferricyanide ion.

several studies have been made of transport processes in devices with a periodic flow passage such as packed beds [17, 18], plate-finned heat exchangers [19, 20] and wavy-walled channels [21–25]. These works focused on the transitional flow at intermediate Reynolds numbers, and all of them found that the transition from steady to unsteady flow occurs at a Reynolds number as low as a few hundred and that fluid motion becomes oscillatory from downstream of a periodic flow passage. The flow transition also leads to heat or mass transfer enhancement.

The principal aim of the present work has been to compare the flow and mass transfer characteristics of transitional flow in a staggered array and an in-line array with the same pitch-to-diameter ratio. Surface shear stress distributions and mass transfer rates were measured by the electrochemical method developed by Mizushina [26]. Flow visualizations were also performed. The effect of tube layout provides insights into the transport processes involved in transitional flow and information useful for the design of compact heat exchangers at intermediate Reynolds numbers.

2. EXPERIMENTAL APPARATUS AND PROCEDURE

The experimental apparatus was the same type of recirculating water tunnel as used in the previous flow and mass transfer studies at high Reynolds numbers [6, 7], with a rectangular duct 160 mm × 80 mm (height × width) as the test section. The acrylic cylinders comprising the array were oriented parallel to the principal walls of the test section, i.e. the upper and lower walls. In both staggered and in-line arrays, 11 rows by 5 columns of cylinders 15 mm in diameter with longitudinal and transverse pitch-to-diameter ratios of two were employed. This choice allowed the experimental results to be compared with those of several numerical studies [5, 16]. The fluid temperature was kept constant by a heat exchanger. The experiment was designed to allow for measurements in the range of Reynolds number ($Re = U_i D/\nu$) that is of particular interest to the transition from steady to unsteady flow, i.e. 50–1000.

Flow was visualized by the aluminium dust method. Perfusion with a suspension of aluminium particles of about 40 μm in diameter enabled us to observe path lines corresponding to streamlines for steady flow. An exposure time of 2 s was selected for aluminium particles to trace paths sufficiently long at low Reynolds numbers of less than 100. Illumination was provided by a 500 W projector.

The surface shear stress and the mass transfer rate in tube banks were measured by an electrochemical method involving measurement of the diffusional current flowing in the electrode circuit when the test electrode is polarized. The test electrode for the shear stress measurements consisted of a platinum wire of 0.5 mm in diameter set on the surface of an acrylic cylinder 15 mm in diameter. The average mass transfer rate was measured with a test electrode consisting of a cylinder of nickel 15 mm in diameter and 20 mm in length inserted in the middle part of an acrylic cylinder of the same diameter. In the present investigation, only one of the tubes in the array was used in the mass transfer measurement, because it seems that the mass transfer is almost identical in all active tubes in a system with high Schmidt numbers. Recently, Ogino *et al.* [27] have confirmed this inference for packed beds using the electrochemical method. The electrolyte solution used contained 0.01 N potassium ferri-ferrocyanide and 1.0 N sodium hydroxide, and its temperature was kept at 25°C (Sc = 1570).

The surface shear stress τ_s and Sherwood number

Sh are related to the diffusional current i_d as follows:

$$\tau_s = 3.55 \times 10^{-15} \mu i_d^3/(C_b^3 d^5 \varphi^2) \quad (1)$$

$$Sh = kD/\varphi = i_d D/(FC_b \varphi A). \quad (2)$$

Special care was taken in all experiments to saturate the electrolyte with nitrogen, block off the test section from light exposure and activate the electrodes.

3. EXPERIMENTAL RESULTS AND DISCUSSION

3.1. *Flow patterns and surface shear stresses*

The details of flow patterns were studied using both still photographs and video tapes. The examples given in this section have been selected to illustrate various flow regimes.

The flow development in the range $60 < Re < 600$ for the staggered array is illustrated in Fig. 1. In each photograph the flow is from left to right, and the tube seen at the centre of each photograph is the third row tube ($N = 3$). At the lowest Reynolds number achievable, $Re = 60$, two stable vortices are formed behind the tube. This behaviour continues up to a Reynolds number of about 110 and is illustrated for $Re = 96$ in the figure. The agreement in terms of the streamlines and the vortex sizes between experimental and numerical results has been confirmed previously [16]. At a Reynolds number of about 120, these vortices become unstable, with flow crossing the wake region of the tube and the vortices periodically being swept in the mainstream flows. As the Reynolds number increases further, the wake region becomes fully turbulent. The photographs at $Re = 300$ and 600 show the influence of the unsteady wakes in perturbing the mainstream flows. The row-by-row variation of the flow patterns is illustrated in Fig. 2 for $Re = 300$. As the flow progresses through the array increasing turbulence is visible. Also the flow pattern around the first row tubes is quite different from that around the third and subsequent row tubes. This is due to the absence of the effect of unsteady wakes at the first row tubes.

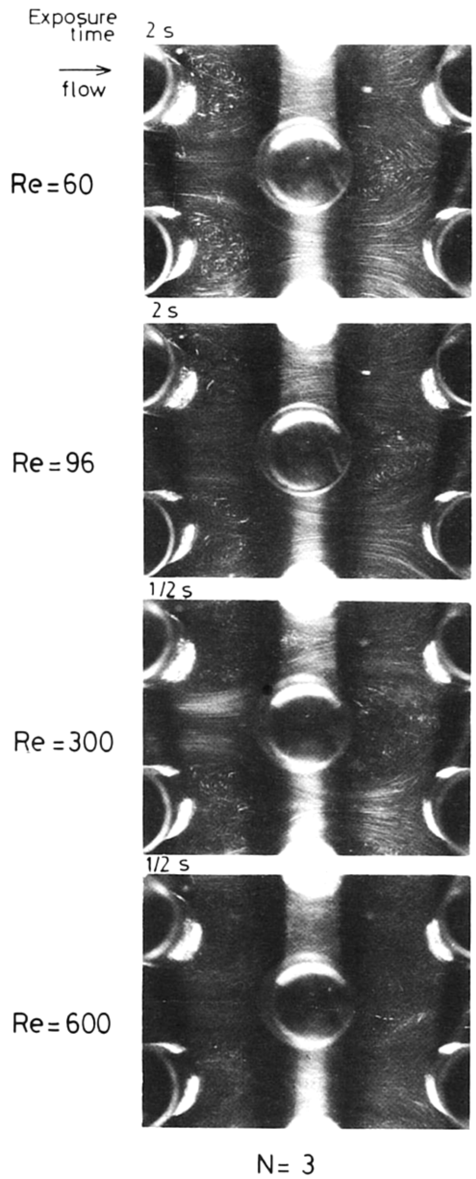

FIG. 1. Effect of Reynolds number on flow patterns for staggered array.

Flow visualization photographs for the in-line array are shown in Figs. 3 and 4. In Fig. 3, the wakes between the third and fourth row tubes consist of two stable vortices with clear straight flow lanes between tube columns until a Reynolds number of about 300, but these vortices become unstable with an increase of Reynolds number. A comparison of Figs. 2 and 4 indicates that the mainstream flows in the staggered array are much more affected by the developing turbulence in the wakes than those in the in-line array.

Flow visualizations allow us to identify different flow regimes, but the frontiers between regimes cannot be determined with precision visually. Therefore, we determined the transition between steady and unsteady flow regimes using a small electrode for the surface shear stress measurement, and also examined the flow behaviour in each regime by signal analysis. The amplitude and frequency of the voltage signals vary around a tube in the array. A selectively amplified frequency is easily visible from the signals of the electrode near $\theta = 90°$, where no flow separation exists. Consequently, the results presented here are from the signals at $\theta = 90°$ for both staggered and in-line arrays.

Figure 5 shows the electrode signals for the last row tube ($N = 11$). For the staggered array shown in Fig. 5(a), the amplitude and the frequencies of the oscillations in the signals are relatively low at $Re = 96$ and increase with the increase of Reynolds number. Sinusoidal waveforms are clearly seen in the signals at $Re = 108$, 165 and 207, indicating that periodic vortex shedding exists just after the transition. Similar results are obtained for the in-line array as shown in

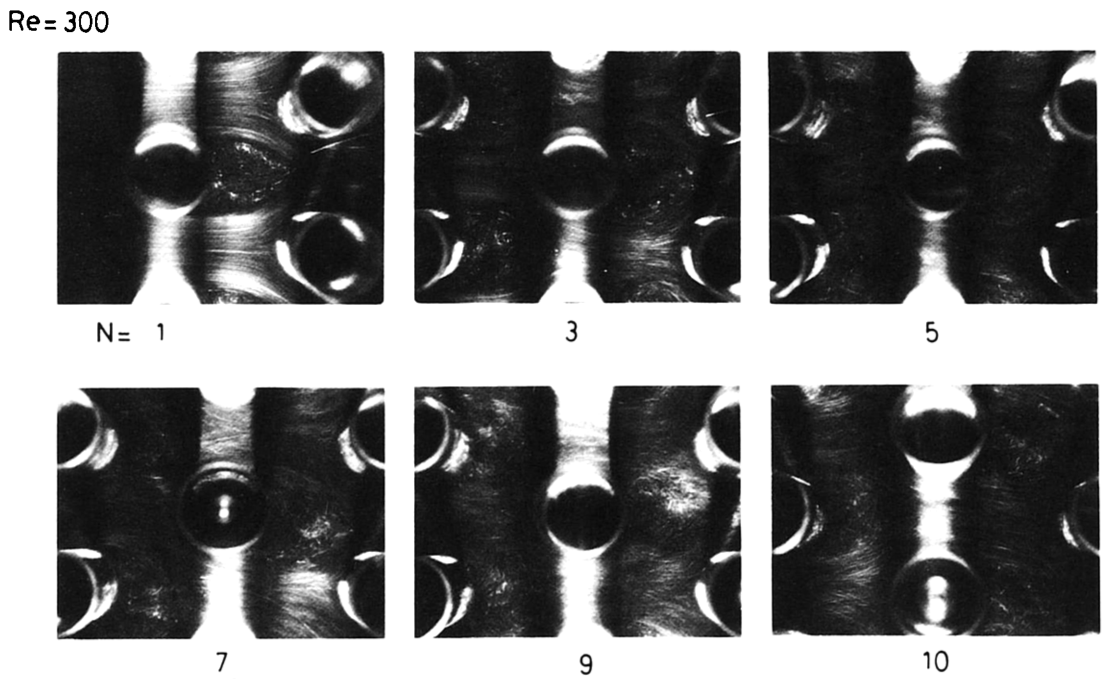

FIG. 2. Row-by-row variation of flow patterns for staggered array at $Re = 300$.

Fig. 5(b), but the amplitudes and the frequencies of the oscillations are quite different. That is, the amplitude is larger for the in-line array than the staggered array, but the frequency is smaller.

Figure 6 shows the signals for an inner row tube of $N = 7$. For the staggered array shown in Fig. 6(a), the variation of signals with Reynolds number is similar to the results for the last row tube of $N = 11$ shown in Fig. 5(a), and thus the critical Reynolds number at the transition is almost identical for $N = 7$ and 11, i.e. $Re_c = 105$. On the other hand, for the in-line array shown in Fig. 6(b), a sinusoidal waveform in the signals at $N = 7$ is not identified until $Re = 140$, and the critical Reynolds number is different for $N = 7$ and 11, i.e. $Re_c = 140$ at $N = 7$ and $Re_c = 105$ at $N = 11$. This finding implies that although the region of flow oscillations spawned by the tubes themselves moves upstream with an increase of Reynolds number, the upstream development of flow transition is much faster for the staggered array than the in-line array. This is probably related to the fact that the frequency of vortex shedding for the staggered array is about two times that for the in-line array as described below.

Figure 7 shows the period of signals corresponding to vortex shedding. The essential features of this figure are that the period of vortex shedding is almost identical for $N = 7$ and 11, and that it is inversely proportional to Reynolds number for both staggered and in-line arrays. Thus the Strouhal number, $St = fD/U_i$ is independent of the row number and the Reynolds number, i.e. $St = 0.559$ for the staggered array and $St = 0.236$ for the in-line array in the Reynolds number range of 100–200. For the vortex shedding in plate arrays, Mochizuki and Yagi [28] have reported that the Strouhal number is independent of the row number of plate fins and the Reynolds number. There is thus a similarity between tube banks and plate arrays. The reason for the small Strouhal number for the in-line array is that the vortex shedding tends to be retarded due to a narrow spacing of tubes in the streamwise direction as compared with the spacing for the staggered array.

Figure 8 shows the surface shear stress distribution at an inner row of $N = 7$ for various Reynolds numbers. The measurements of the time-averaged absolute values of the surface shear stress are represented by the dimensionless surface vorticity, ζ_s. The solid line in this figure denotes the numerical result for $Re = 54$ [16]. The agreement between the experimental and numerical shear stresses is good, thus confirming the validity of the shear stress measurement by the electrochemical method. At the front of the tube ($\theta = 0°$–$60°$), the dimensionless surface shear stresses vary approximately as the 0.5 power of the Reynolds number, indicating the existence of laminar boundary layer flow according to boundary layer theory. In particular, it should be noted that the laminar boundary layer flow is maintained even for unsteady flow at high Reynolds numbers. Thus the surface shear stress is insensitive to the unsteady wakes of the preceding row tubes. The surface shear stresses at the rear of the tube ($\theta = 120°$–$180°$) are considerably smaller than those at the front even for unsteady flow.

Figure 9 shows the results for the in-line array. The

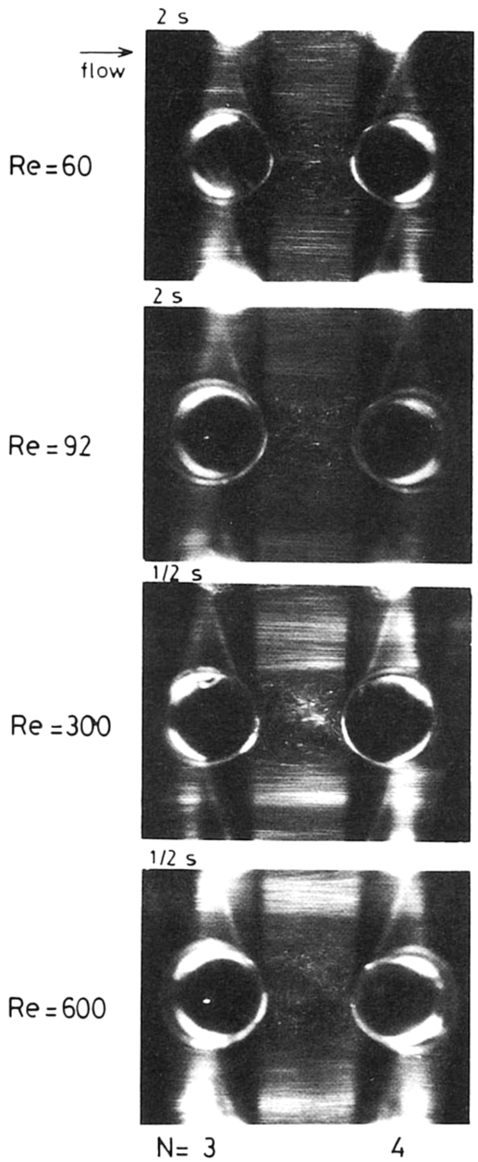

FIG. 3. Effect of Reynolds number on flow patterns for in-line array.

shear stresses at the front of the tube ($\theta = 0$–40°) are smaller than for the staggered array in the steady flow regime. However, they increase significantly after the flow becomes unsteady. This phenomenon is not observed for the staggered array and reveals that the unsteady wakes of the preceding row tubes are responsible for the increment of the shear stress of the subsequent row tubes for the in-line array. At the rear of the tube ($\theta = 120$–180°), the behaviour of shear stresses for the in-line array is almost identical to that for the staggered array.

In addition, for both staggered and in-line arrays, the shear stresses at all row numbers show similar variations with Reynolds number except for the first row, as expected from the flow visualizations.

3.2. *Mass transfer rates*

The average mass transfer rates at an inner row of $N = 7$ for both staggered and in-line arrays are presented in Fig. 10 as $Sh/Sc^{1/3}$ vs Re_{max}. Re_{max} is based on the pitch velocity at the minimum flow area between tubes and in this case is related to Re through the simple relationship $Re_{max} = 2Re$. The solid line in the figure is the mass transfer correlation at $N = 1$. The mass transfer rates at $N = 1$ are independent of the layout of tubes and increase monotonically with Reynolds number.

The mass transfer rate at $N = 7$ for the staggered array is almost equal to that at $N = 1$ in the steady flow regime ($Re_{max} < 210$). However, it gradually departs from that at $N = 1$ with increasing Reynolds number after the flow becomes unsteady. Thus the mass transfer is sensitive to the unsteady wakes of the preceding row tubes, while the shear stress is insensitive to such wakes as shown in Fig. 8. Similar results have been found for mass transfer between a plane surface and an impinging turbulent jet by Kataoka *et al.* [29]. There is thus a striking similarity between the impinging jet flow structure and that described for the staggered array: in both cases the flow in the boundary layer is accelerated with a steep negative gradient of the surface pressure.

The mass transfer rate at $N = 7$ for the in-line array is smaller than that at $N = 1$ in the steady flow regime ($Re_{max} < 280$) and also smaller than that for the staggered array, as expected from comparison of the shear stress distributions of Figs. 8 and 9. However, after the flow transition, the mass transfer rate increases markedly in the Reynolds number range of 500–1000 and reaches that for the staggered array at higher Reynolds numbers. This result corresponds well with the variation of the shear stress distributions with Reynolds number shown in Fig. 9. Thus the increment of the mass transfer is due to the unsteady wakes of the preceding row tubes. Similar results have been obtained for two cylinders in tandem in cross flow [30].

The row-by-row variation of the mass transfer rate is illustrated in Figs. 11 and 12. This is small for the staggered array even after the flow transition, as shown in Fig. 11, but for the in-line array as shown in Fig. 12, it is considerable in the Reynolds number range of 200–2000 although the mass transfer rate is independent of the row number at higher Reynolds numbers than 3000. The mass transfer difference between the staggered and in-line arrays is due to the faster upstream development of flow transition for the staggered array than the in-line array, as found in the signal analysis of Figs. 5 and 6. The upstream development of heat transfer enhancement with increasing Reynolds number has also been observed in fin arrays of large thickness [20]. There is thus a striking similarity between tube banks and fin arrays: in both cases upstream development of flow transition due to vortex shedding leads to heat or mass transfer enhancement.

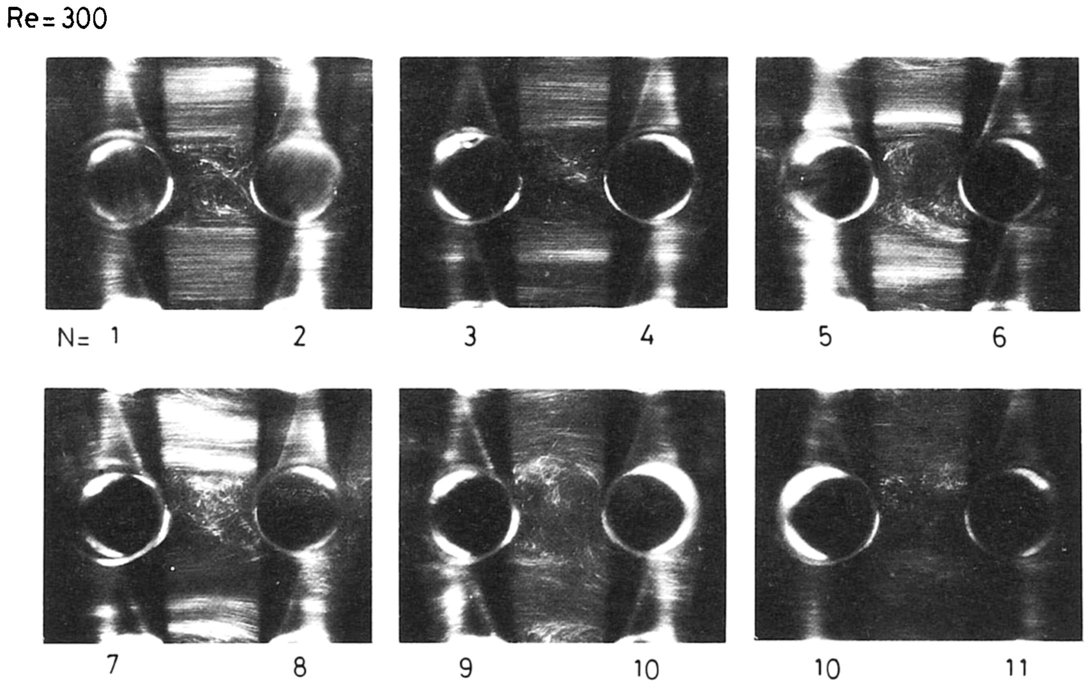

FIG. 4. Row-by-row variation of flow patterns for in-line array.

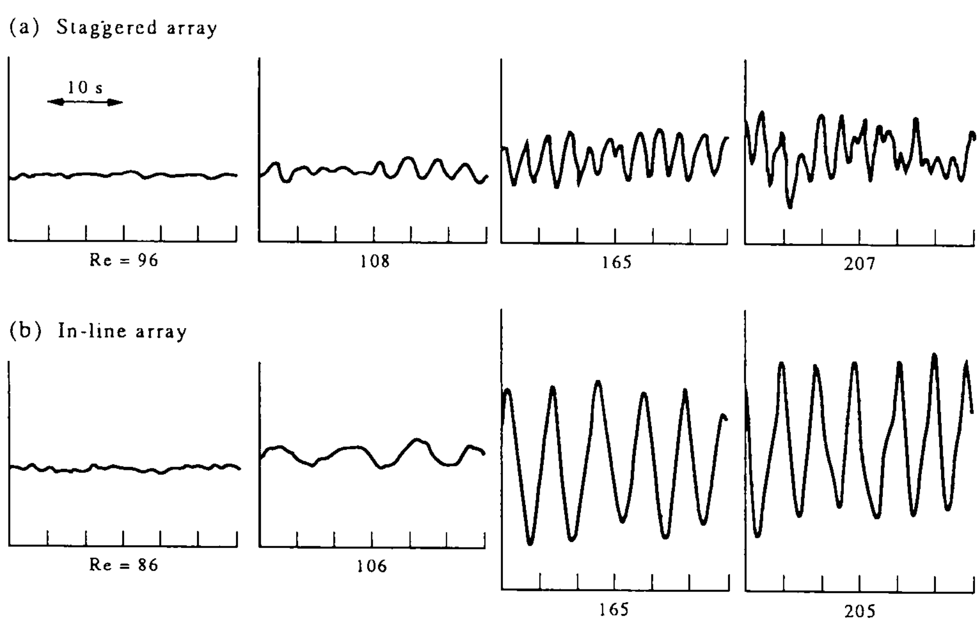

FIG. 5. Characteristic signals representing vortex shedding from tubes at $N = 11$.

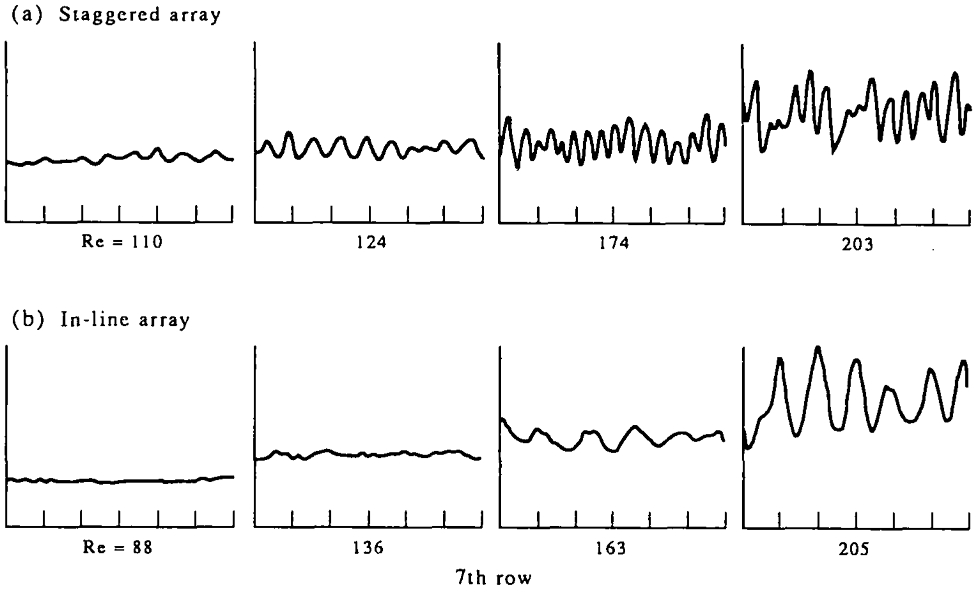

FIG. 6. Characteristic signals representing vortex shedding from tubes at $N = 7$.

Comparison of the present results with those of the literature, as $Sh/Sc^{1/3}$ vs Re_{max}, is shown in Figs. 13(a) and (b) for in-line and staggered arrays, respectively. The agreement with other experimental studies [31–33] is satisfactory as a whole although the orders of Schmidt number or Prandtl number are different. In particular, the present data agree well with the correlations at high Reynolds numbers ($Re_{max} > 2000$) by Nishimura [31] because the Schmidt numbers are the same. Recently, heat transfer in tube banks for pitch-to-diameter ratio of two has been predicted under steady laminar flow conditions using the finite analytic method by Chen and Wung [5]. In Fig. 13 the numerical results are also presented for comparison. For the in-line array, the agreement with the numerical predictions is good at low Reynolds numbers ($Re_{max} < 200$), but the experimental data are higher than the numerical predictions at higher Reynolds numbers. This is because vortex shedding is not considered in the computation while in the experiment the shedding appears. For the staggered array, similar results are observed although the agreement with the numerical correlation is not good at low Reynolds numbers. Thus the effect of vortex shedding has to be considered in numerical calculations for the prediction of heat or mass transfer as the fluid motion becomes oscillatory.

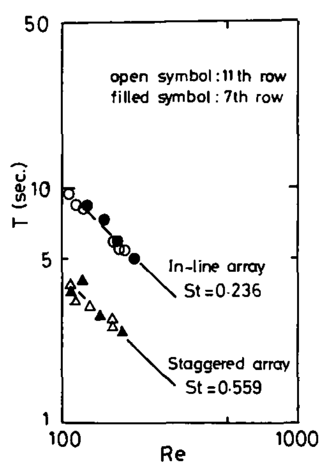

FIG. 7. Period of vortex shedding vs Reynolds number.

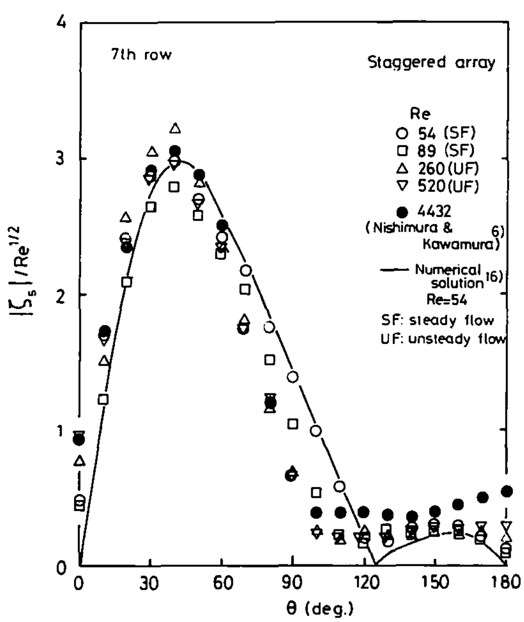

FIG. 8. Surface shear stress distribution for various Reynolds numbers at $N = 7$ for staggered array.

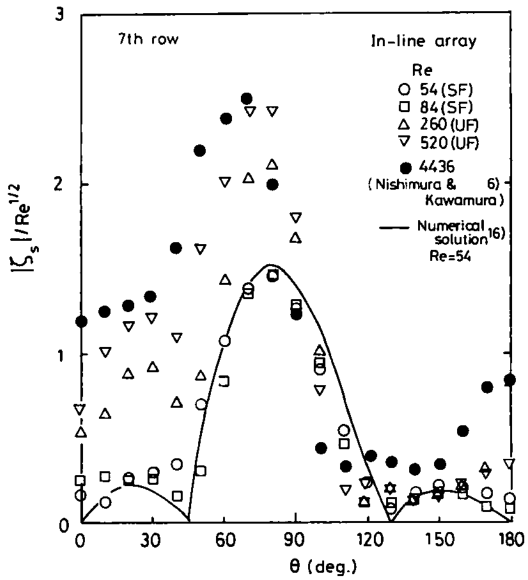

FIG. 9. Surface shear stress distribution for various Reynolds numbers at $N = 7$ for in-line array.

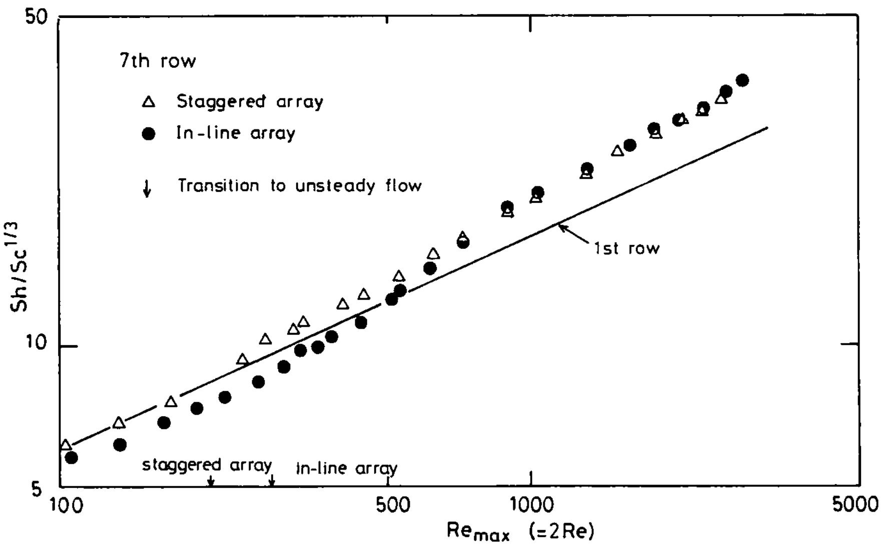

FIG. 10. Average Sherwood numbers at $N = 7$ for staggered and in-line arrays.

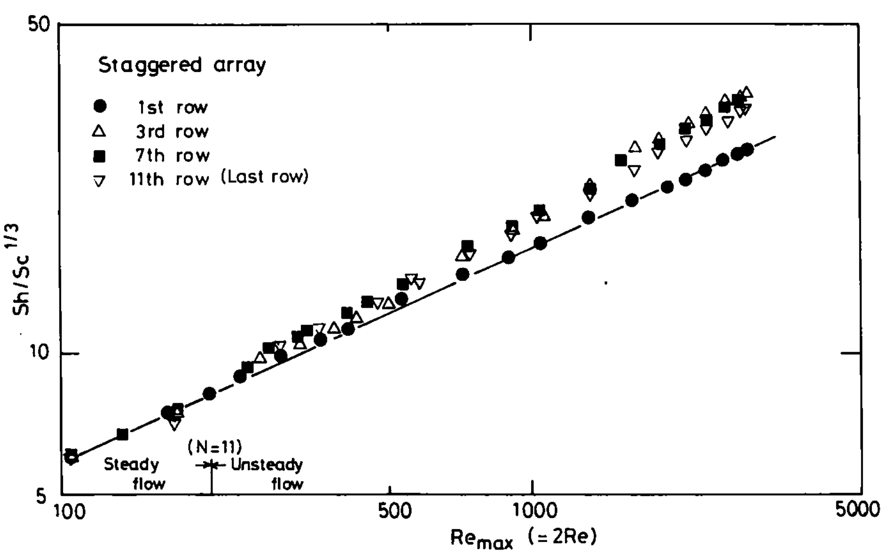

FIG. 11. Row-by-row variation of Sherwood number for staggered array.

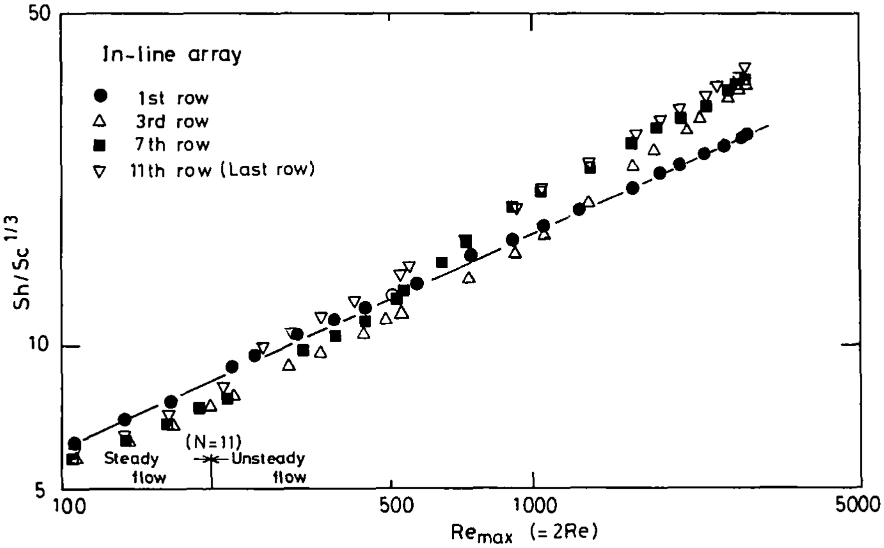

FIG. 12. Row-by-row variation of Sherwood number for in-line array.

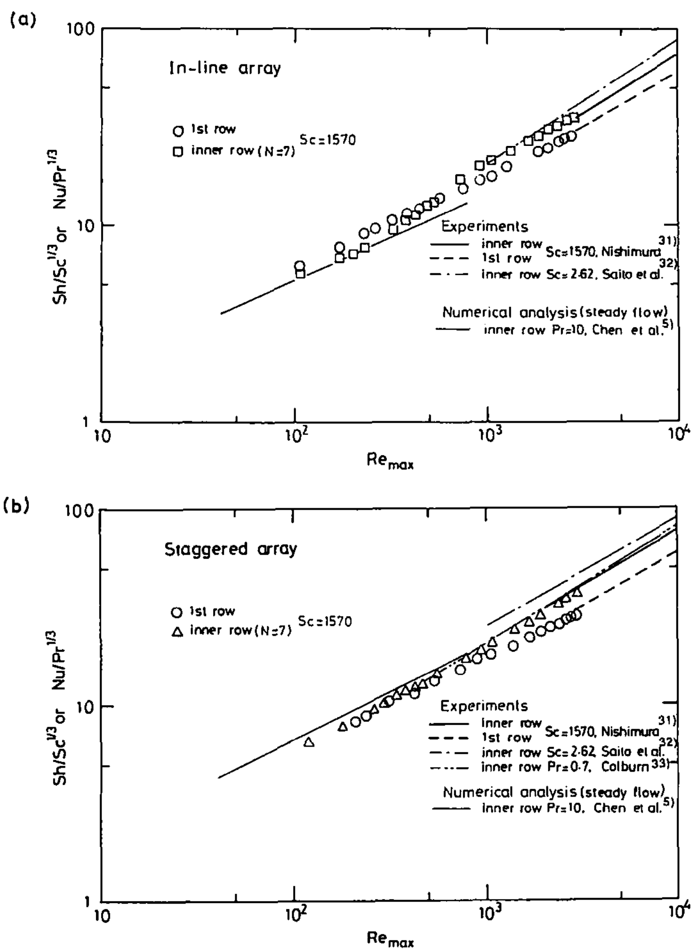

FIG. 13. Comparison with previous studies on the correlation of Sherwood number and Reynolds number for pitch-to-diameter ratio of two.

4. CONCLUSIONS

Flow and mass transfer characteristics were compared for a staggered array and an in-line array with the same pitch-to-diameter ratio of two at the transition from steady to unsteady flow. The following conclusions are drawn.

(1) The upstream development of flow transition due to vortex shedding is much faster for the staggered array than the in-line array. Therefore, the row-by-row variation of the mass transfer rate is smaller in the staggered array than the in-line array.

(2) For the staggered array, the mass transfer is sensitive to the unsteady wakes of the preceding row tubes, while the surface shear stress is insensitive to such wakes. For the in-line array, the mass transfer and shear stress are both sensitive to the unsteady wakes.

(3) The Strouhal number representing vortex shedding from tubes in the array is independent of both the row number and the Reynolds number, i.e. $St = 0.559$ for the staggered array and $St = 0.236$ for the in-line array in the Reynolds number range of 100–200.

Acknowledgements—The authors express their appreciation to Emeritus Professor Yuji Kawamura of Hiroshima University for his kind interest and encouragement, and also acknowledge with thanks the assistance of graduate student Kazuhiro Ohya of Toyama University in the experiments.

REFERENCES

1. A. A. Zukauskas, Heat transfer from tubes in cross-flow. In *Advances in Heat Transfer* (Edited by T. P. Irvine, Jr. and J. P. Hartnett), Vol. 8, pp. 93–160. Academic Press, New York (1972).
2. T. Nishimura, Flow across tube banks. In *Encyclopedia of Fluid Mechanics* (Edited by N. P. Cheremisinoff), Vol. 1, pp. 763–785. Gulf, Houston (1986).
3. S. Aiba, Heat transfer of closely-spaced tube banks, *J. Heat Transfer Soc. Jap.* **27**, 70–87 (1988).
4. Y. Chang, A. N. Beris and E. E. Michaelides, A numerical study of heat and momentum transfer for tube bundles in crossflow, *Int. J. Numer. Meth. Fluids* **8**, 1381–1394 (1989).
5. C. J. Chen and T. S. Wung, Finite analytic solution of convective heat transfer for tube arrays in cross-flow: Part II—Heat transfer analysis, *Trans. ASME J. Heat Transfer* **111**, 641–648 (1989).
6. T. Nishimura and Y. Kawamura, Flow pattern in tube banks in the fully developed region, *Kagaku Kogaku Ronbunshu* **7**, 222–227 (1981).
7. T. Nishimura and Y. Kawamura, Mass transfer in tube banks in the fully developed region, *Heat Transfer—Jap. Res.* **10**, 82–95 (1981).
8. S. Aiba, H. Tsuchida and T. Ota, Heat transfer around tubes in in-line banks, *Bull. JSME* **25**, 919–926 (1982).
9. S. Aiba, H. Tsuchida and T. Ota, Heat transfer around tubes in staggered tube banks, *Bull. JSME* **25**, 927–933 (1982).
10. K. A. Antonopoulos, Heat transfer in tube banks under conditions of turbulent inclined flow, *Int. J. Heat Mass Transfer* **28**, 1645–1656 (1985).
11. M. J. Schuh, C. A. Schuler and J. A. C. Humphrey, Numerical calculation of particle laden gas flows past tubes, *A.I.Ch.E. Jl* **35**, 466–480 (1989).
12. A. Zukauskas and R. Ulinskas, Efficiency parameters for heat transfer in tube banks, *Heat Transfer Engng* **6**, 19–25 (1985).
13. I. A. Nieva and U. Böhm, Local mass transfer for cross flow through tube banks of square in-line layout at intermediate Reynolds numbers, *Int. J. Heat Mass Transfer* **26**, 1283–1288 (1983).
14. I. A. Nieva and U. Böhm, Local mass transfer for cross flow through tube banks: equilateral triangular layout at intermediate Reynolds numbers, *Int. Commun. Heat Mass Transfer* **12**, 277–285 (1985).
15. D. S. Weaver and A. Abd-Rabbo, A flow visualization study of a square array of tubes in water crossflow, *Trans. ASME J. Fluid Engng* **107**, 354–363 (1985).
16. T. Nishimura, H. Itoh, K. Ohya and H. Miyashita, Experimental validation of numerical analysis of flow across tube banks for laminar flow, *J. Chem. Engng Jap.* **24**, 666–669 (1991).
17. A. J. Karabelas, T. H. Wegner and T. J. Hanratty, Flow pattern in a close-packed cubic array of spheres near the critical Reynolds number, *Chem. Engng Sci.* **28**, 673–682 (1973).
18. M. A. Latifi, N. Midoux, A. Storck and J. N. Genoe, The use of micro-electrodes in the study of the flow regimes in a packed bed reactor with single phase liquid flow, *Chem. Engng Sci.* **44**, 2501–2508 (1989).
19. S. Mochizuki, Y. Yagi and W. J. Yang, Flow pattern and turbulence intensity in stacks of interrupted parallel-plate surfaces, *Exp. Thermal Fluid Sci.* **1**, 51–57 (1988).
20. G. N. Xi, K. Suzuki, Y. Hagiwara and T. Murata, Experimental study on heat transfer characteristics of offset fin arrays: effect of fin thickness in the low and middle ranges of Reynolds number, *Trans. JSME, Ser. B* **55**, 3507–3514 (1989).
21. T. Nishimura, Y. Kajimoto, A. Tarumoto and Y. Kawamura, Flow structure and mass transfer for a wavy channel in transitional flow regime, *J. Chem. Engng Jap.* **19**, 449–455 (1986).
22. T. Nishimura, S. Murakami, S. Arakawa and Y. Kawamura, Flow observations and mass transfer characteristics in symmetrical wavy-walled channels at moderate Reynolds numbers for steady flow, *Int. J. Heat Mass Transfer* **33**, 835–845 (1990).
23. T. Nishimura, K. Yano, T. Yoshino and Y. Kawamura, Occurrence and structure of Taylor–Goertler vortices induced in two-dimensional wavy channels for steady flow, *J. Chem. Engng Jap.* **23**, 697–703 (1990).
24. K. D. Stephanoff, Self-excited shear-layer oscillations in a multi-cavity channel with a steady mean velocity, *Trans. ASME J. Fluid Engng* **108**, 338–342 (1986).
25. M. Greiner, R. F. Chen and R. A. Wirtz, Heat transfer augmentation through wall-shape-induced flow destabilization, *Trans. ASME J. Heat Transfer* **112**, 336–341 (1990).
26. T. Mizushina, The electrochemical method in transport phenomena. In *Advances in Heat Transfer* (Edited by T. P. Irvine, Jr. and J. P. Hartnett), Vol. 7, pp. 87–161. Academic Press, New York (1971).
27. F. Ogino, M. Kamata and K. Mukai, Mass transfer in a slit-type packed bed, *Proc. 28th Natn. Heat Transfer Symp. Jap.*, D124 (1991).
28. S. Mochizuki and Y. Yagi, Characteristics of vortex shedding in plate arrays. In *Flow Visualization II* (Edited by W. Merzkirch), pp. 99–103. Hemisphere, Washington, DC (1982).
29. K. Kataoka, Y. Kamiyama, S. Hashimoto and T. Komai, Mass transfer between a plane surface and an impinging turbulent jet: the influence of surface-pressure fluctuations, *J. Fluid Mech.* **119**, 91–105 (1982).

30. T. Nishimura, Y. Ohori and Y. Kawamura, Flow pattern and rate of mass transfer around two cylinders in tandem, *Int. Chem. Engng* **26,** 123–129 (1986).
31. T. Nishimura, Transport phenomena in closely-spaced tube banks, Ph.D. Thesis, Hiroshima University, Japan (1981).
32. H. Saito and K. Kishinami, Analogy between heat and mass transfer in tube banks, *Heat Transfer—Jap. Res.* **1,** 96–103 (1972).
33. A. P. Colburn, A method of correlating forced convection heat transfer data and a comparison with fluid friction, *Trans. A.I.Ch.E.* **29,** 174–209 (1933).